Pulse propagation dynamics in the presence of a continuous-wave field

2013 Phys. Scr. 2013 014011

(http://iopscience.iop.org/1402-4896/2013/T157/014011)

Phys. Scr. **T157** (2013) 014011 (4pp) doi:10.1088/0031-8949/2013/T157/014011

Pulse propagation dynamics in the presence of a continuous-wave field

Jelena Dimitrijević, Dušan Arsenović and Branislav M Jelenković

Institute of Physics, University of Belgrade, Pregrevica 118, 10080 Belgrade, Serbia

E-mail: jelena.dimitrijevic@ipb.ac.rs

Received 20 August 2012
Accepted for publication 18 December 2012
Published 15 November 2013
Online at stacks.iop.org/PhysScr/T157/014011

Abstract

We present theoretical results for the propagation dynamics of an electromagnetic field pulse through rubidium vapor, while another field, a continuous-wave electromagnetic field, is present. The frequencies of both electromagnetic fields are resonant with the transition between the ground and excited state hyperfine levels of Rb, $F_g \rightarrow F_e = F_g \pm 1$. Detuning from resonance is done by the magnetic field oriented along the light propagation direction (Hanle configuration). When both the electromagnetic fields are simultaneously interacting with Rb atoms, either electromagnetically induced transparency or absorption is induced. Propagation dynamics was obtained solving the set of Maxwell–Bloch equations for the interacting atoms with two electromagnetic fields. Motivated by recent results (Brazhnikov *et al* 2011 *Eur. Phys. J.* D **63** 315–25; Brazhnikov *et al* 2010 *JETP Lett.* **91** 625–9; Kou *et al* 2011 *Phys. Rev.* A **84** 063807), we have analyzed the influence of experimental parameters, laser polarization, and mutual phases between lasers, which can lead to optical switching, i.e. the transformation from electromagnetically induced absorption to transparency and vice versa.

PACS numbers: 42.50.Gy, 42.50.Nn

(Some figures may appear in color only in the online journal)

1. Introduction

Laser–atom interactions, which can develop coherent phenomena in atoms, electromagnetically induced transmission (EIT) [1] and absorption (EIA) [2] in alkali atoms, have attracted a great deal of interest in recent decades because of the important applications of both the phenomena. For such coherences to develop, lasers have to couple the long-lived ground state hyperfine level(s) with the excited hyperfine level(s) of alkali atoms. Narrow EIT and EIA resonances and steep dispersion in the narrow spectral bandwidth of the resonances are the unique properties of atomic systems in which the propagation of laser pulses can be considerably slowed or completely blocked [6–8]. Studying the dynamics of laser pulses in coherent media is of interest for all optical switchings [9, 10], squeezed light [11], quantum information science, etc.

Different atomic schemes can be applied in order to induce EIT or EIA. This can be the pump–probe configuration when two lasers couple two hyperfine (or two Zeeman) levels with the common excited hyperfine level in either Λ (two levels belong to the ground state) or V (levels belong to the excited state) atomic schemes. In the Hanle configuration, a single laser couples Zeeman sublevels of hyperfine levels of alkali atoms. Raman detuning in the latter case is done by applying a proper magnetic field.

In this paper, we analyze the mutual effects of two laser fields on their propagation, when both the laser fields induce simultaneously either EIT or EIA in the Rb vapor. The specific case when one laser is continuous wave (CW) and the other is pulsed is analyzed. We show how lasers' coherent interactions can be manipulated by appropriately changing the mutual orientation of their polarization vectors and their relative phases. So far, very little has been done to investigate the mutual effects of propagation of a laser pulse in a coherently prepared medium when a CW laser, which makes the preparation, is present.

2. Theoretical model

We solve the set of Maxwell–Bloch equations (MBEs) for the interaction of two lasers, one of which is pulsed and

the other is CW, with Rb atoms. The frequencies of both lasers are adjusted to either $F_g = 2 \rightarrow F_e = 3$ or $F_g = 2 \rightarrow F_e = 1$ transition, where we solve MBEs for the full atomic systems of both transitions, i.e. for all Zeeman sublevels. The parameters for the transitions in Rb, used in calculations, were taken from [12, 13]. The evolution of the density matrix $\hat{\rho}$ is calculated from the optical Bloch equations

$$\frac{\mathrm{d}\hat{\rho}(t)}{\mathrm{d}t} = -\frac{\mathrm{i}}{\hbar}[\hat{H}_0, \hat{\rho}(t)] - \frac{\mathrm{i}}{\hbar}[\hat{H}_1, \hat{\rho}(t)] - \hat{\mathrm{SE}}\hat{\rho}(t) - \gamma\hat{\rho}(t) + \gamma\hat{\rho}_0. \tag{1}$$

Diagonal elements of $\hat{\rho}$, ρ_{g_i,g_i} and ρ_{e_i,e_i} are populations, ρ_{g_i,g_j} and ρ_{e_i,e_j} are Zeeman coherences and ρ_{g_i,e_j} and ρ_{e_i,g_j} are optical coherences, where indices g and e stand for the ground and excited sublevels.

We solve MBEs for different values of the magnetic field B_s, as described by the Hamiltonian $\hat{H}_0$. The quantization axis is chosen parallel to the direction of the magnetic field $\mathbf{B}_s$ which is also the direction along which the lasers propagate. The energies due to the Zeeman splitting are given by $E_{g(e)} = \mu_B l_{F_{g(e)}} m_{g(e)} B_s$, where $m_{g(e)}$ are the magnetic quantum numbers of the ground and excited sublevels, μ_B is the Bohr magneton and $l_{F_{g,e}}$ is the Lande gyromagnetic factor for two hyperfine levels. $\hat{\mathrm{SE}}$ stands for the abbreviated spontaneous emission operator with the rate Γ. The relaxation of all density matrix elements, due to the finite time for an atom to cross the laser beam, is given by the term $\gamma\hat{\rho}$, while $\gamma\hat{\rho}_0$ takes into account the continuous flux of atoms entering laser beams with equal population of the ground Zeeman sublevels. The role of laser detuning (and Doppler broadening) is not discussed here.

$\hat{H}_I$ is the interaction Hamiltonian describing the coherent interaction of the laser fields with atoms. The electric field vector represents the sum of two electric fields:

$$\vec{E}(t,z) = \sum_l [E_x^l \cos(\omega^l t - k^l z + \varphi_x^l)\vec{e}_x + E_y^l \cos(\omega^l t - k^l z + \varphi_y^l)\vec{e}_y], \tag{2}$$

where $l = 1, 2$ stands for the pulsed and CW lasers. E^l are the amplitudes of two fields, ω^l are their angular frequencies, $\omega^l = \pm ck^l$, and c is the speed of light. k^l are lasers' wave vectors, where we take $k^l > 0$ for the propagation along the positive direction of the z-axis. In equation (2), E_x^l, E_y^l are the real Descartes components of the amplitude of the electric field and φ_x^l, φ_y^l are the associated phases, also real quantities. The electric field vector can further be written as

$$\vec{E}(t,z) = \sum_l [\mathrm{e}^{\mathrm{i}(\omega^l t - k^l z)}\vec{u}_{+1}E_{++}^l + \mathrm{e}^{\mathrm{i}(\omega^l t - k^l z)}\vec{u}_{-1}E_{-+}^l + \mathrm{e}^{-\mathrm{i}(\omega^l t - k^l z)}\vec{u}_{+1}E_{+-}^l + \mathrm{e}^{-\mathrm{i}(\omega^l t - k^l z)}\vec{u}_{-1}E_{--}^l], \tag{3}$$

where the following substitution has been introduced:

$$E_{++}^l = \frac{-E_x^l \mathrm{e}^{+\mathrm{i}\varphi_x^l} + \mathrm{i}E_y^l \mathrm{e}^{+\mathrm{i}\varphi_y^l}}{2\sqrt{2}}, \quad E_{+-}^l = \frac{-E_x^l \mathrm{e}^{-\mathrm{i}\varphi_x^l} + \mathrm{i}E_y^l \mathrm{e}^{-\mathrm{i}\varphi_y^l}}{2\sqrt{2}},$$
$$E_{-+}^l = \frac{E_x^l \mathrm{e}^{+\mathrm{i}\varphi_x^l} + \mathrm{i}E_y^l \mathrm{e}^{+\mathrm{i}\varphi_y^l}}{2\sqrt{2}}, \quad E_{--}^l = \frac{E_x^l \mathrm{e}^{-\mathrm{i}\varphi_x^l} + \mathrm{i}E_y^l \mathrm{e}^{-\mathrm{i}\varphi_y^l}}{2\sqrt{2}}. \tag{4}$$

In equation (4), E_{++}^l, E_{+-}^l, E_{-+}^l, E_{--}^l are the complex amplitudes of the fields and the relation $(E_{++}^l)^* = -E_{--}^l$, $(E_{+-}^l)^* = -E_{-+}^l$ stands.

The usual substitution for the optical coherences

$$\rho_{g_i,e_j} = \sum_l \mathrm{e}^{\mathrm{i}(\omega^l t - k^l z)}\tilde{\rho}_{g_i,e_j}^i, \quad \rho_{e_i,g_j} = \sum_l \mathrm{e}^{-\mathrm{i}(\omega^l t - k^l z)}\tilde{\rho}_{e_i,g_j}^l \tag{5}$$

has been introduced, where the sum is taken over lasers that couple states g_i and e_j. This substitution means that we are working in line with the multi-mode Floquet theory [14] for the case of counter-propagating lasers, or with the single-mode one for the case of lasers with the same frequency. We use the approximation with the zeroth-order harmonics for the ground-state and the excited-state density matrix elements and up to the first-order harmonics for the optical coherences.

The propagation dynamics of the electric-field amplitudes, for the propagation along the positive direction of the z-axis, is given by MBEs:

$$\left(\frac{\partial}{\partial z} + \frac{1}{c}\frac{\partial}{\partial t}\right)E_{\pm+}^l = -\mathrm{i}\frac{k^l N_c}{2\varepsilon_0}P_{\pm+}^l,$$
$$\left(\frac{\partial}{\partial z} + \frac{1}{c}\frac{\partial}{\partial t}\right)E_{\pm-}^l = +\mathrm{i}\frac{k^l N_c}{2\varepsilon_0}P_{\pm-}^l \tag{6}$$

and for the propagation along the negative direction of the z-axis, MBEs stand:

$$\left(-\frac{\partial}{\partial z} + \frac{1}{c}\frac{\partial}{\partial t}\right)E_{\pm+}^l = -\mathrm{i}\frac{k^l N_c}{2\varepsilon_0}P_{\pm+}^l,$$
$$\left(-\frac{\partial}{\partial z} + \frac{1}{c}\frac{\partial}{\partial t}\right)E_{\pm-}^l = \mathrm{i}\frac{k^l N_c}{2\varepsilon_0}P_{\pm-}^l. \tag{7}$$

In equations (6) and (7), new quantities were introduced which are calculated as

$$P_{++}^l = \sum_{g_i \leftrightarrow e_j} \tilde{\rho}_{g_i,e_j}^l \mu_{g_i,e_j,+1}, \quad P_{+-}^l = \sum_{e_i \leftrightarrow g_j} \tilde{\rho}_{e_l,g_j}^l \mu_{g_i,e_j,+1},$$
$$P_{-+}^l = \sum_{g_i \leftrightarrow e_j} \tilde{\rho}_{g_i,e_j}^l \mu_{g_i,e_j,-1}, \quad P_{--}^l = \sum_{e_i \leftrightarrow g_j} \tilde{\rho}_{e_i,g_j}^l \mu_{g_i,e_j,-1}, \tag{8}$$

where the sum is taken over the dipole-allowed transitions induced by lasers. These four variables appear in the components of macroscopic polarization of the atomic medium which is calculated as $\vec{P}(t,z) = N_c e\,\mathrm{Tr}[\hat{\rho}\hat{\vec{r}}]$ or

$$\vec{P}(t,z) = N_c \sum_l [\mathrm{e}^{\mathrm{i}(\omega^l t - k^l z)}(\vec{u}_{+1}P_{++}^l + \vec{u}_{-1}P_{-+}^l) + \mathrm{e}^{-\mathrm{i}(\omega^l t - k^l z)}(\vec{u}_{+1}P_{+-}^l + \vec{u}_{-1}P_{--}^l)]. \tag{9}$$

3. Results and discussion

3.1. Effect of the polarization of two laser fields

We present the results for the propagation dynamics of two lasers propagating through the Rb vapor. One is the CW laser, another is the pulsed laser and both couple the same Rb transition. Recent results [3, 4] showed that, for the two counter-propagating CW fields, it is possible to reverse

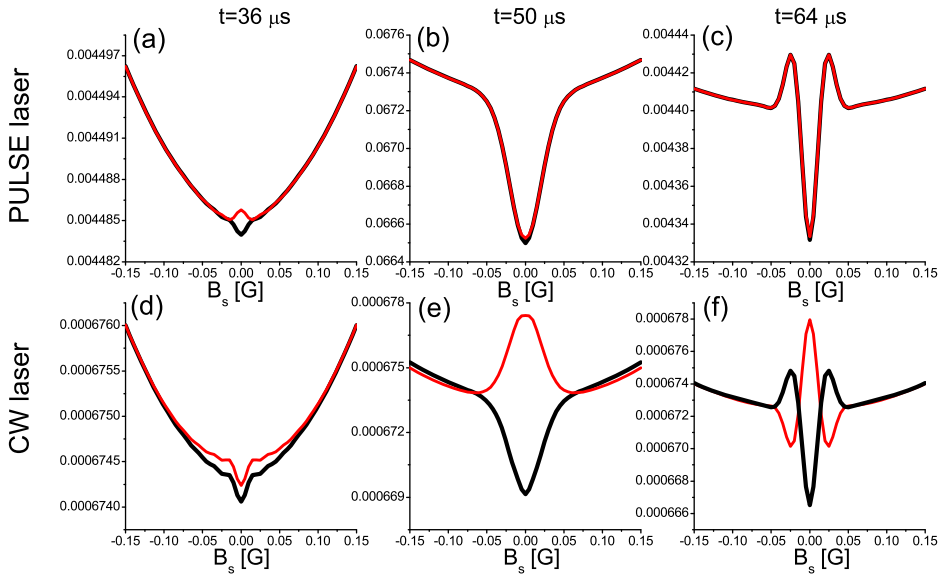

Figure 1. Transmission of the pulse (top row) and the CW laser (bottom row) for three different moments: $t = 36\,\mu$s (a, d), $t = 50\,\mu$s (b, e) and $t = 64\,\mu$s (c, f). Black curves show the results when the polarization vectors of both lasers are parallel, $\theta_{\rm CW} = 0$, and red curves show transmissions when the polarization vector of the CW field is rotated, $\theta_{\rm CW} = \frac{\pi}{2}$.

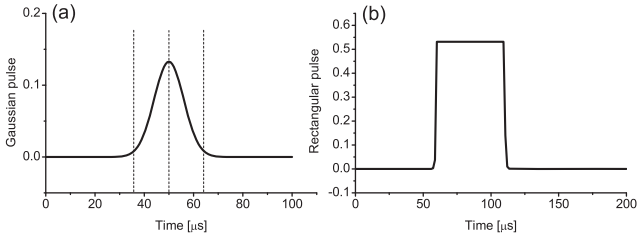

Figure 2. Waveforms of laser pulses used in the calculations: a Gaussian pulse (a) and a rectangular pulse (b). Dashed vertical lines in panel (a) indicate moments for which we present the results in figure 1.

the sign of the resonance by a purely polarization method. They performed numerical and analytical calculations for the simple three-level schemes. Both lasers couple the $F_{\rm g} = 2 \rightarrow F_{\rm e} = 3$ transition in ^{87}Rb, and each can independently induce EIA in the vapor. We analyze how the counter-propagating pulse affects the properties of a CW laser, and the other way around, how the existence of the CW laser changes the properties of the propagating laser pulse. Transmissions of lasers are calculated for values of the external magnetic field near zero, i.e. around the EIA resonance. Calculations were performed by solving the set of MBEs (see section 2) for the same transition. Both lasers are linearly polarized, and we study the effects of different angles between their polarization vectors on the propagation of both lasers.

In figure 1, we present the transmissions of both lasers for two different values of the angle of rotation of the CW laser polarization vector ($\theta_{\rm CW}$). The temporal shape of the pulse is Gaussian $I^0_{\rm pulse} {\rm e}^{-\frac{(t-t_0)^2}{\sigma^2}}$ (see figure 2(a)), where $\sigma = 10\,\mu{\rm s}/\sqrt{2\ln 2}$. The intensity of the laser pulse, at the peak of the amplitude, $t_0 = 50\,\mu$s, is $I^0_{\rm pulse} = 1.327\,21 \times 10^{-2}\,{\rm mW\,cm^{-2}}$. The intensity of the CW laser at the entrance of the cell is $I^0_{\rm CW} = 10^{-2} I^0_{\rm pulse}$. We take the relaxation due to the time of flight to be $\gamma = 0.001\Gamma$, where $\Gamma = 2\pi\ 6.066\,62 \times 10^6$ Hz is the spontaneous emission rate. The density of Rb atoms in the cell is $N_{\rm c} = 10^{14}\,{\rm m^{-3}}$ and the length of the cell is 0.1 m. The results in figure 1 are given for three moments of time: when the pulse is entering the cell, $t = 36\,\mu$s, when its peak intensity is in the cell, $t = 50\,\mu$s, and when it is leaving the cell, $t = 64\,\mu$s. The positions of these three moments with respect to the pulse are indicated in figure 2(a) with vertical dashed lines.

When the polarizations of both lasers are parallel, $\theta_{\rm CW} = 0$ (black curves in figure 1), the transmissions of both lasers show EIA resonances at all instants, as expected for the lasers locked to the $F_{\rm g} = 2 \rightarrow F_{\rm e} = 3$ transition. Rotation of the polarization vector of the CW laser by $\pi/2$ yields different transmission profiles of the CW laser. At the time moment $t = 36\,\mu$s, when the pulse starts entering the cell, the transmission of the CW laser is not influenced by the pulse's presence in the cell and shows small EIA for both values of $\theta_{\rm CW}$ (see figure 1(d)). As the pulse's intensity increases, the atomic ensemble gets affected by both lasers' fields. Results in figure 1(e) show that at time $t = 50\,\mu$s, due to the rotated polarization of the CW field, the transmission of the CW laser completely changes the sign of resonance from EIA (black curve, $\theta_{\rm CW} = 0$) to EIT (red curve, $\theta_{\rm CW} = \frac{\pi}{2}$). Under the simultaneous action of both lasers, depending on the mutual angle between their linear polarizations, the CW laser can change the sign of resonance, allowing our system to act as an optical switch for the CW laser. Specific profiles of the transmissions of both lasers at the time moment $t = 64\,\mu$s (figures 1(c) and (e)) are due to residual, long-lived coherences, after the pulse's passing through the cell.

The transmission of the pulse laser does not change with $\theta_{\rm CW}$ during most of the pulse's passage through the cell (see figures 1(a)–(c)), since with our choice of parameters the pulse's intensity is much larger than that of the CW field, $I^0_{\rm pulse} = 10^2\, I^0_{\rm CW}$. The sign reversal in figure 1(a) happens since, at that time instant, the lasers are nearly at the same magnitude of intensity. Results where we present the optical switching of the pulse's transmission will be published elsewhere.

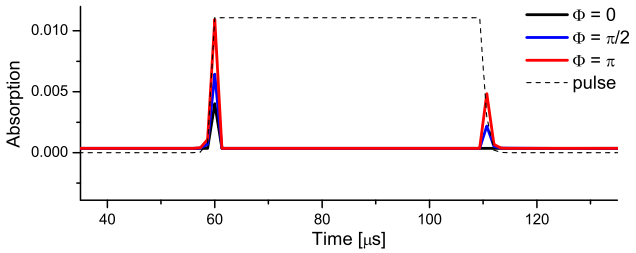

Figure 3. Total absorption of both lasers for three different values of the initial phase of the σ^- component of the pulse laser. The phases of the other three σ components are 0. Given by the dashed line is the waveform of the pulse laser, normalized to the maximum value of absorptions.

3.2. Effect of the relative phase between laser fields

We have analyzed the effects of different initial phases of the two lasers. In the recent analysis by Kou *et al* [5], similar effects were studied, except that they used two pulsed lasers (or four σ components) and MBEs were solved for the simple three-level scheme. In our analysis, we analyze the mutual effects of a linearly polarized pulse and a CW laser. Here we assume that the lasers are co-propagating and are locked to the $F_g = 2 \rightarrow F_e = 1$ transition, thus inducing the dark state and EIT. We solve MBEs for this transition, assuming a single mode for the substitution, given by equation (5), since all σ components have the same frequency. The absorption of the two lasers is calculated as a function of different initial phases of the lasers' σ waves.

We solve MBEs for the CW and the pulse laser assuming a near-rectangular pulse for the pulsed laser (see figure 2(b)). The edges of the pulse are approximated by the exponential rise and fall slopes in order to introduce a more realistic situation:

$$\text{pulse} = \begin{cases} I^0_{\text{pulse}}\, \mathrm{e}^{-s(t-t_2)}, & t > t_2, \\ \mathrm{e}^{s(t-t_1)}, & t > t_1, \\ 1, & t_1 \leqslant t \leqslant t_2, \end{cases} \tag{10}$$

where the slope is given by $s = 2 \times 10^6$ Hz, the intensity of the pulse's σ component is $I^{\sigma 0}_{\text{pulse}} = 0.053\,088\,4\,\text{mW cm}^{-2}$, and the beginning and the end of the pulse are $t_1 = 60\,\mu$s and $t_2 = 110\,\mu$s, respectively. Relaxation due to the time of flight is taken as $\gamma = 10^{-6}\,\Gamma$, where $\Gamma = 2\pi \times 5.750\,06 \times 10^6$ Hz is the spontaneous emission rate. The concentration of atoms in the cell is $N_c = 10^{14}\,\text{m}^{-3}$ and the cell's length is 0.1 m. The intensity of the CW laser's σ components is $I^{\sigma 0}_{\text{CW}} = 10^2 I^{\sigma 0}_{\text{pulse}}$. The results presented here are given for the magnetic field $B = 0$.

In figure 3 we present the total absorption of all four σ components from both lasers, from the time when the pulse laser is applied until the end of the pulse. Results are given for three different values of the initial phase of the σ^- component of the pulse laser (Φ), while the initial phases of other σ components are kept constant. From figure 3, we see that the rapid change of absorptions is happening only during the transient regime when the pulse laser is turned on and off.

In this configuration, the CW laser plays the role of a pumping laser, preparing the atoms into the dark state. Before the pulse laser is turned on, the absorption of the CW laser is nearly zero, due to the EIT. When the pulse laser is turned on, a new dark state is formed. This leads to a quick change in absorption of laser fields, until a new superposition of atomic levels, this time under the action of both lasers, generates a new dark state for both electromagnetic fields, and consequently the new EIT and minimal absorption. The reverse situation happens when the pulse laser is turned off. The results in figure 3 show that the absorption of two lasers strongly depends on their initial phases. Similarly to Kou *et al* [5], we have shown the considerable phase dependence for the case of a combined pulse and CW laser field.

4. Conclusions

We have theoretically analyzed the propagation dynamics of two laser fields: when the pulse laser enters the Rb cell while another, the CW laser, is present. Both lasers couple the same two hyperfine levels, of the ground and excited states of Rb. We studied the case when both can induce either dark or bright resonances, leading to EIT or EIA. We have shown that, with an appropriate choice of parameters (polarization direction and mutual phases) and geometry (counter and co-propagating lasers), both fields affect each other's behavior while propagating through the Rb vapor. This type of coherent manipulation of atoms can lead to magneto-optical switching techniques or optical-storage devices. Our numerical analysis is applied to the realistic system, that is, the Rb atom, and as such indicates that these phenomena can be observable in realistic experiments by using the alkali–metal atoms.

Acknowledgments

This work was supported by the Ministry of Education, Science and Technological Development of the Republic of Serbia under grant number III 45016.

References

[1] Arimondo E 1996 *Prog. Opt.* **35** 257–354
[2] Akulshin A M, Barreiro S and Lezama A 1998 *Phys. Rev.* A **57** 2996
[3] Brazhnikov D V, Taichenachev A V and Yudin V I 2011 *Eur. Phys. J.* D **63** 315–25
[4] Brazhnikov D V, Taichenachev A V, Tumaikin A M, Yudin V I, Ryabtsev I I and Entin V M 2010 *JETP Lett.* **91** 625–9
[5] Kou J, Wan R G, Kang Z H, Jiang L, Wang L, Jiang Y and Gao J Y 2011 *Phys. Rev.* A **84** 063807
[6] Novikova I, Phillips D F and Walsworth R L 2007 *Phys. Rev. Lett* **99** 173604
[7] Okuma J, Hayashi N, Fujisawa A and Mitsunaga M 2009 *Opt. Lett.* **34** 1654–6
[8] Boyer V, McCormick C F, Arimondo E and Lett P D 2007 *Phys. Rev. Lett.* **99** 143601
[9] Li J, Yu R, Si L and Yang X 2010 *J. Phys. B: At. Mol. Opt. Phys.* **43** 065502
[10] Qi Y, Niu Y, Zhou F, Peng Y and Gong S 2011 *J. Phys. B: At. Mol. Opt. Phys.* **44** 085502
[11] Imad H Agha, Christina Giarmatzi, Quentin Glorieux, Thomas Coudreau, Philippe Grangier and Gaétan Messin 2011 *New J. Phys.* **13** 043030
[12] Steck D A 2010 Rubidium 85 D, Line Data (http://steckus/alkalidata) (revision 2.1.4, 23 December 2010)
[13] Steck D A 2010 Rubidium 87 D, Line Data (http://steckus/alkalidata) (revision 2.1.4, 23 December 2010)
[14] Chu S I and Telnov D A 2004 *Phys. Rep.* **390** 1–131